

AD-A068 773

COLUMBIA UNIV DOBBS FERRY N Y HUDSON LABS

F/G 17/1

PHASE SPREADING IN DIRECTLY TRANSMITTED SOUND-WAVE PACKETS, (U)

JUN 66 N W LORD

NONR-266(84)

UNCLASSIFIED

108

NL

| OF |
AD
A068773

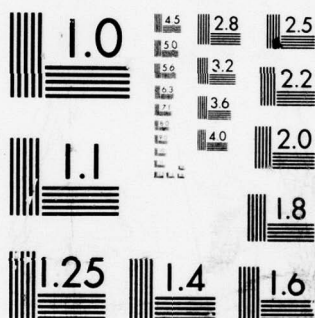
AD
A068773

AD
A068773

AD
A068773



END
DATE
FILMED
6 --79
DDC



MICROCOPY RESOLUTION TEST CHART
NATIONAL BUREAU OF STANDARDS-1963-A

1
COLUMBIA UNIVERSITY
HUDSON LABORATORIES
CONTRACT Nonr-266(84)

Hudson Laboratories ✓
of
Columbia University
Dobbs Ferry, New York 10522

8
PHASE SPREADING IN DIRECTLY TRANSMITTED
SOUND-WAVE PACKETS††

by

10 Norman W. Lord

11 16 Jun 66

12 14 p.

D D C
DECLASSIFIED
MAY 21 1979
A
A
DISTRIBUTION STATEMENT A
Approved for public release;
Distribution Unlimited

14 * Hudson Laboratories of Columbia University Informal Documentation
No. 198

† Presented at the Seventy-first Meeting of the Acoustical Society of
America, Boston, Massachusetts, June 1-4, 1966. 123

† This work was supported by the Office of Naval Research under Contract
15 Nonr-266(84)

79 05 02

~~79 05 02 28 05 0~~
172 050

ABSTRACT

A short sound pulse, transmitted horizontally between two points in deep ocean water, arrives at the receiver as a continuous superposition of time-separated wave packets. This fact has been demonstrated by a detailed analysis of the cross covariance between such pulses carrying a phase reversal and a truncated replica. In all, about 280 pulses were selected from over 3000 which were previously studied (N. W. Lord, J. Acoust. Soc. Am., 36, 1043 (A), 1964) for the transmission-time fluctuation. For these 1200 cps pulses the phase spreading becomes tangible at a range of 7 km where it is approximately $\frac{\pi}{3}$, or about 0.2 msec. As an estimate of instantaneous phase spread, this value is reasonable compared to the transmission-time fluctuation, for this range, of 0.7 msec between pulses spaced every 0.6 sec. The use of a truncated replica on a long pulse depresses most of the side-lobe cross-covariance peaks. The magnitude of the central peak is related to both the phase spreading and the chosen length of the truncated replica, although this latter dependence is lost by a slow phase reversal. Hence, for these measurements, if Δ is the phase spread, the magnitude of the cross-covariance peak is $(\sin \Delta) / \Delta$. At ranges under 7 km, Δ is small and the peak is close to unity with small fluctuation. At ranges over 7 km the peak declines and fluctuates more among the successive pulses.

ABSTRACT NO.	
NTIS	DATE INDEXED
DOC	REF. NUMBER
ANALYST'S NAME	
INSTITUTION	
BY	
ENTRUSTMENT/REMARKS/DOCS	
FILE	ANAL. INFO. / SECTION
A	

Two years ago I presented a study of the transmission-time fluctuations suffered by short sound pulses that had been transmitted horizontally through a heterogeneous medium, fairly deep ocean water. This is illustrated in Fig. 1, which represents the relative sound velocity by shadings, light for high, dark for low.

From such a standpoint the transmission time is regarded, to a first approximation, as changing by virtue of the movement of this patchy medium across the sound path. In the present report I will show that even a single sound pulse can experience the existing heterogeneity in a demonstrable way; in this case, of course, the effect exists even if the medium is static.

The experiment as shown in Fig. 2, was carried out with sound levels maintained at a very high signal-to-noise level by using a highly directional source. Both source and receiver were maintained in a small depth range centered at 800 meters. Very sensitive timing was obtained by placing an abrupt reversal in phase in the middle of a short pulse and recording both source and far-field signals on the same magnetic tape.

It is this phase reversal that provides the basis for a new kind of analysis, one that systematically describes these distortions of waveform that are due solely to spatial heterogeneity of the medium. In the simple direct presentations of the received waveform as shown in Fig. 3, we see explicit examples of this distortion that, for statistically significant groups of pulses, will increase with the range.

The bow hydrophone is only 200 ft from the source, and we can assume that the waveform received on it is free of distortion. Although the time scales in Fig. 4 are different, these tracings clearly show the

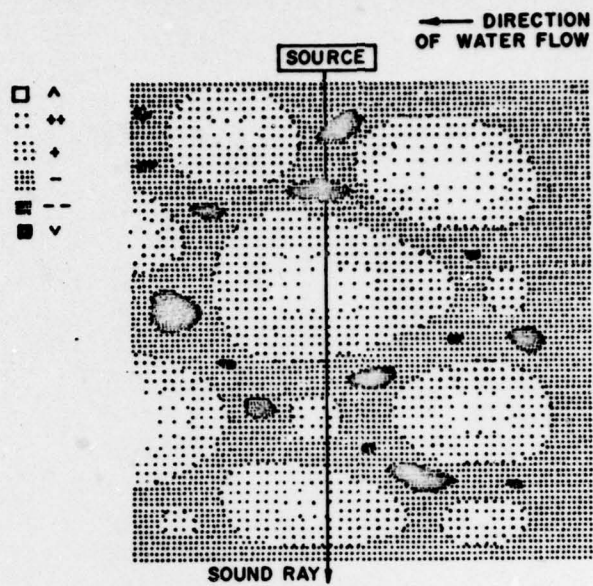


Figure 1

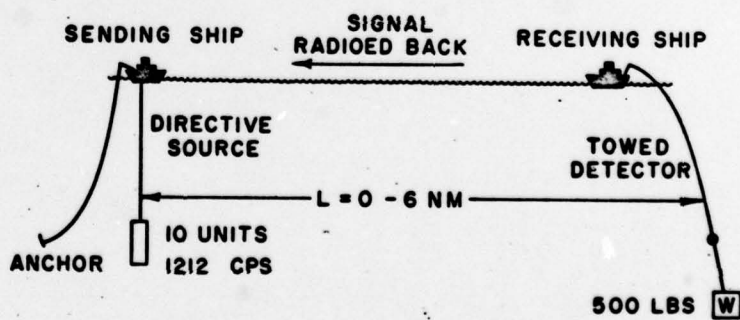


Figure 2

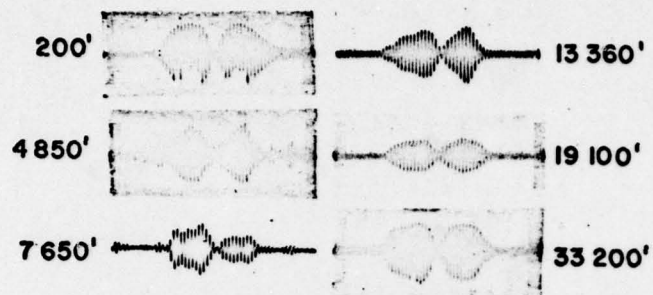


Figure 3

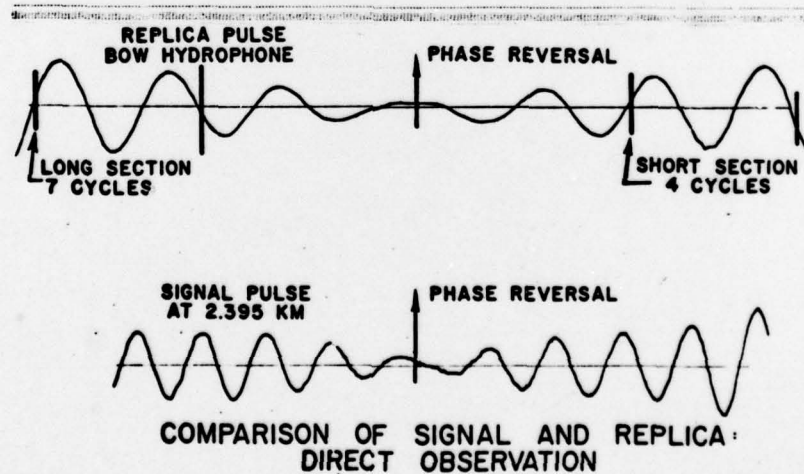


Figure 4

slight distortion in a close-range signal waveform, which is evident in the asymmetry of the small central undulation.

On another point bear in mind the apparent change in the successive peaks moving out from the phase reversal instant that is due to the slow response of the transducers.

The treatment of small waveform distortions embodies several assumptions that may not always be met in reality but, if that is so, are clearly recognizable. To begin with I assume that the received waveform is composed of a quasi-continuous narrow distribution of wavelets whose individual travel times are tightly clustered about one clear average as in this particular illustration. Very frequently, but much less than a tenth of the time, the distribution is much too badly split into several peaks. On the other hand, when the assumption is valid, it can be shown with computer-calculated models that the appearance of the waveform is highly independent of the distribution's shape and reflects indiscriminately its second moment. In my analysis we consider a rectangular shape and use its half-width as our indicator.

First we can represent phase reversals shown in Fig. 5 as wave trains, $P(\theta)$, which carry the factor, F . In the case of $\mu = 0$ we define the convolution of the two waveforms as

$$SD = \int_{-\pi}^{+\pi} \sin^2 \theta \, d\theta = \pi$$

For ν greater than zero, but less than π , we segment the integral to compute

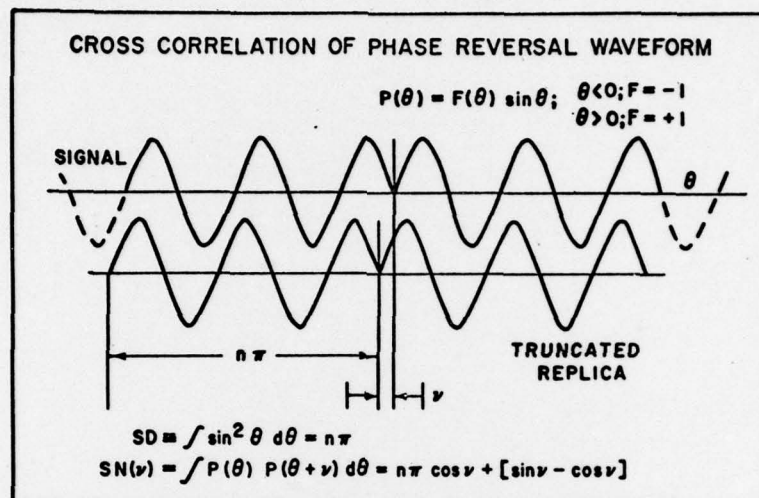


Figure 5

$$\begin{aligned}
SN(\nu) &= \int_{-\pi\pi-\nu}^{+\pi\pi-\nu} \sin\theta \sin(\theta+\nu) d\theta - 2 \int_{-\nu}^0 \sin\theta \sin(\theta+\nu) d\theta \\
&= \pi\pi \cos \nu + [\sin \nu - \nu \cos \nu]
\end{aligned}$$

the two terms being contributed to separately by the two integrals.

Then the cross covariance of our waveforms is the quotient of $SN(\nu)$ by SD as shown in Eq. 1.

$$CCV(\nu) = \frac{SN(\nu)}{SD} = \cos \nu + \frac{1}{\pi\pi} [\sin \nu - \nu \cos \nu] \quad (1)$$

For small ν less than a radian, the bracketed term is positive. As ν grows it oscillates with increasing amplitude. However, for values greater than $\pi\pi$, the segmentation of the integral must be changed. Actually from then on, of course, the cross covariance is zero for an ideal case.

We can now consider our realistic case of the superposition of wave packets with very small mutual phase separations that we represent as a rectangular distribution over $\pm \Delta$. Then we have the equation

$$\sum_0^{\Delta} (\Delta) = \int \frac{CCV(\nu)}{\Delta} d\nu = \frac{\sin \Delta}{\Delta} + \frac{1}{\pi\pi\Delta} [2 - 2 \cos \Delta - \Delta \sin \Delta] \quad (2)$$

with the following numerical table for the dependence on Δ stated in units of l , where $\Delta = \frac{fl\pi}{2}$ and the length of the truncated replica as $2\pi\pi$ is stated in units of n .

n \ l					
	0	$\frac{2}{\pi}$	1	2	3
4	1	.847	.660	.102	-.099
7	1	.845	.650	.058	-.147

Relation between Peak Cross-Covariance, $\sum_0 (\Delta)$ and
Phase Spread, Δ

If we look carefully at Fig. 4, comparing the replica and signal waveform, it is evident that one can represent the successive changes in the peaks by changes in the value of F subscripted for each half cycle, as follows:

$$\begin{array}{ll}
 P(\theta) = F(\theta) \sin \theta: & \theta < -6\pi & F_{i \leq -6} = -4 \\
 & -6\pi < \theta < -4\pi & F_{-5, -4} = -3 \\
 & -4\pi < \theta < -2\pi & F_{-3, -2} = -2 \\
 & -2\pi < \theta < 0 & F_{-1, 0} = -1 \\
 & 0 < \theta < 2\pi & F_{+0, +1} = +1 \text{ etc.}
 \end{array}$$

For example in the case of the long replica, $n = 7$, the integral SD is evaluated as

$$SD \equiv 2 \sum_{n_i} \int_{n_i}^{n_i + \pi} F_i^2 \sin^2 \theta d\theta = 14\pi \left[\underbrace{1.4 + 2.3^2 + 2.2^2 + 2.1^2}_{44} \right]$$

Since the big terms of each integral in the cross-covariance quotient remain equal to each other, the main change introduced here is in the small bracketed term of $SN(v)$, i.e., $[\sin v - v \cos v]$ appears only for $|i| < 2$. This leads through an approximate calculation for \sum_0 to these new values which differ from the values of the earlier slide by only a few thousandths.

$$\sum_0 (\Delta) \text{ for } \Delta = 1 \text{ Radian}$$

$$n = 4 : .842$$

$$n = 7 : .841$$

We can now look briefly at Figs. 6-9 showing typical results when we cross correlate our signal with a truncated replica. At the lowest range we don't see much loss from unity for \sum_0 . It is true that the long replica peak should be lower but not that much lower for small phase spread. In fact such a discrimination is beyond the resolving power of these measurements. Note how in Fig. 7 the order is reversed.

In Fig. 8 we begin to see a more tangible phase-spreading effect and actually here the near equality of the two replica results is a much better consistency than either of the low-range cases.

Finally in Fig. 9 we have an example at the farthest range and although \sum_0 has dropped considerably, as we expect for increased phase spreading, we also have too high a relative value for the long replica. This happened quite often, and I have no explanation for it.

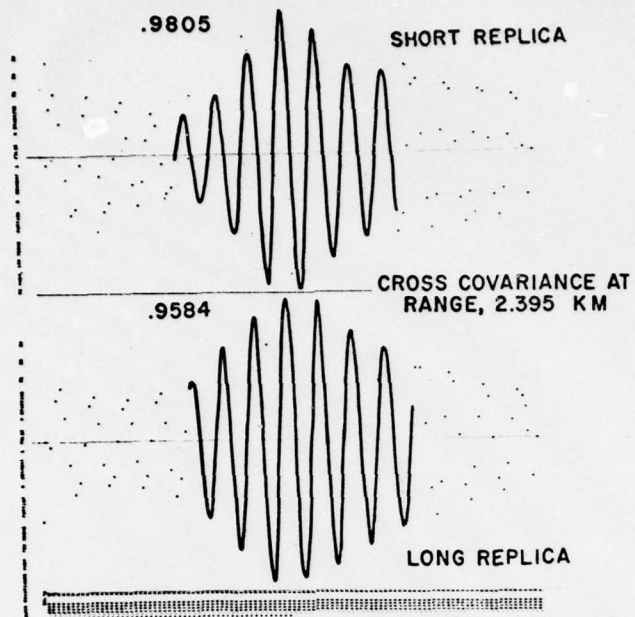


Figure 6

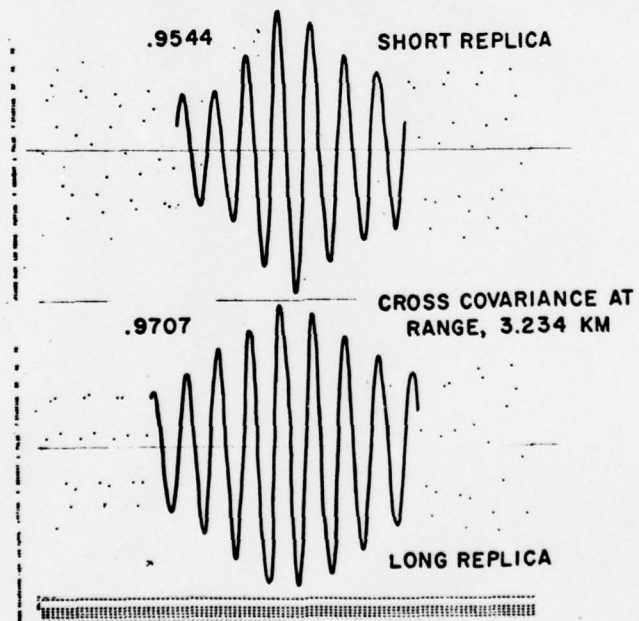


Figure 7

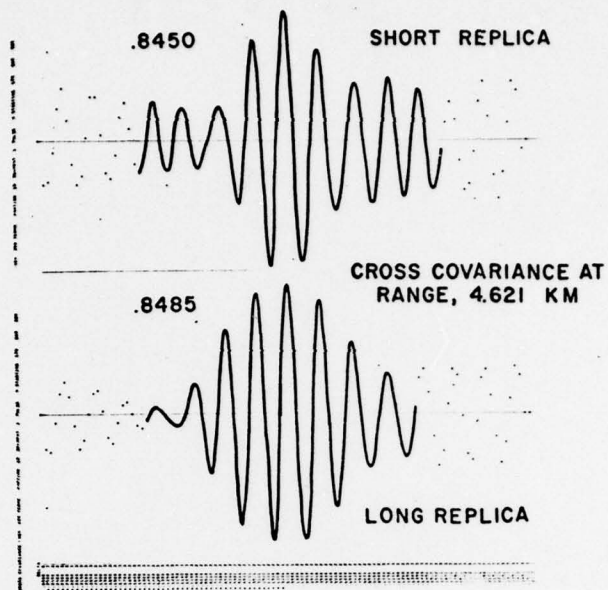


Figure 8

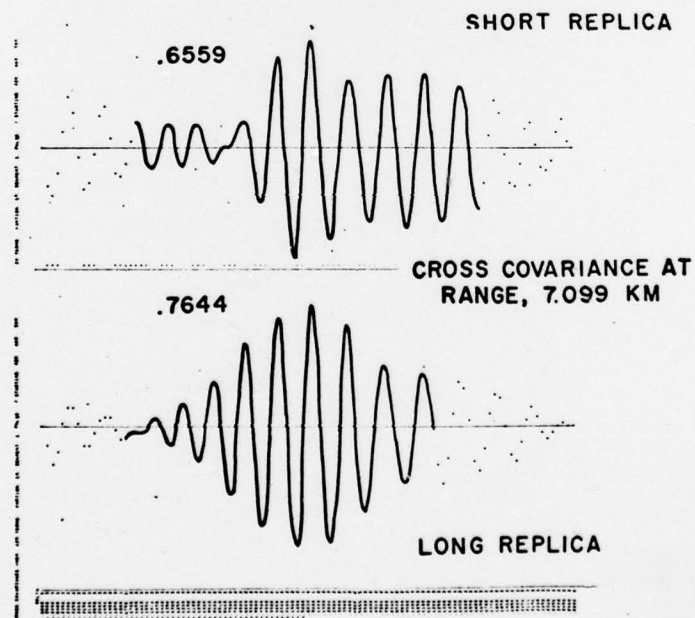


Figure 9

The comparison in Table I between phase spread and transit-time fluctuations shows a definite correlation as we go out in range. Figures like 0.05 msec for phase spread probably represent a basic noise level for this rather old data. We can certainly expect, as range is increased and the sound beam is confined within a much larger cross section of the medium that the spreading goes up. However it must also be recognized as strongly dependent on the particular ray path involved.

For all the ranges considered in this particular experiment the average ray path conforms closely to that shown in Fig. 10. The similar depth of 800 meters for source and receiver, with the velocity profile minimum considerably below this, insures that the path must bend against the almost linear thermocline. Certainly this is so for a maximum height of bent path that is no more than 250 meters.

This maximum height is an index of both how much the path may bend and change transit time between successive pulses and also how big in vertical width would be the effective beam cross section. While the very few points obtained are no solid evidence, we certainly see a qualitative conformity with a square law dependence upon the range that would match the behavior of the horizontal ray height as shown in Fig. 11.

THIS PAGE IS BEST QUALITY PRACTICABLE
FROM COPY FURNISHED TO DDC

CCV Statistics
25 - Pulse Samples

Avg. Range (KM.)	Short Avg. Peak	Replica RMS DEV	Long Avg. Peak	Replica RMS DEV	Estim. Phase Spread (MS.)	250 - Pulse Samples Transit Time Fluct. (MS.)
2.049	.965	.015	.970	.018	.06	.39
2.395	.973	.010	.976	.014	.05	.30
3.234	.970	.016	.974	.018	.05	.37
4.621	.921	.027	.920	.022	.09	.41
7.099	.518	.162	.591	.092	.24	.69

Comparison of Phase Spread and
Transit Time Fluctuations

Table I

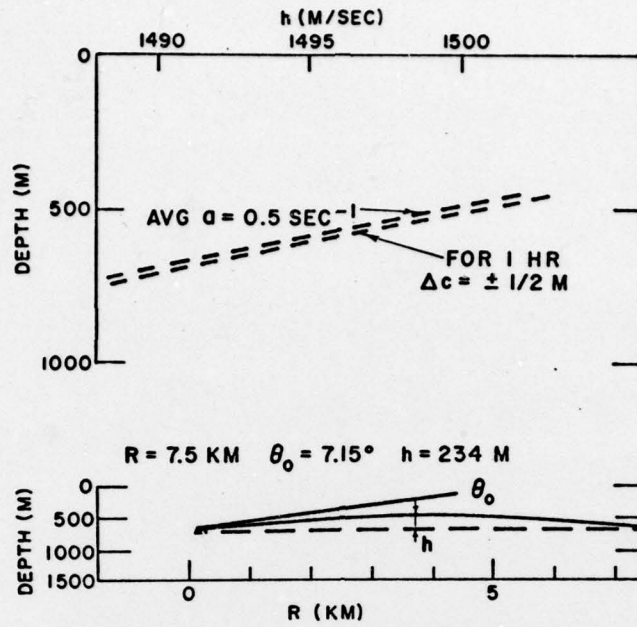


Figure 10

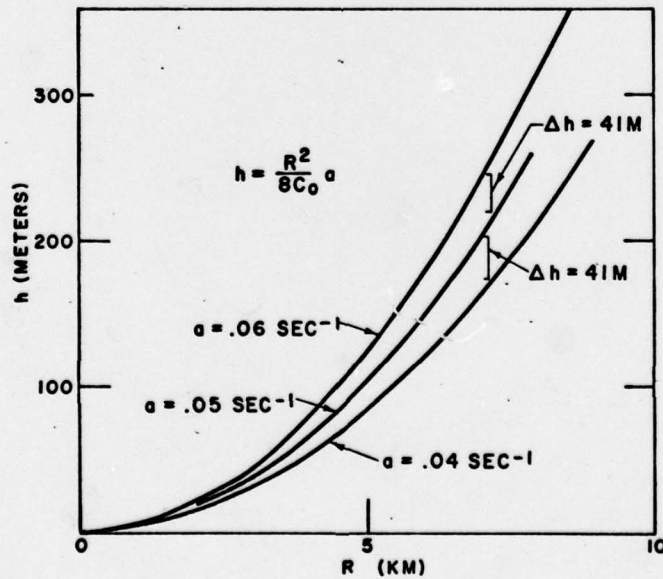


Figure 11